Submitted to The ISME Journal

Bacterioplankton taxa compete for iron along the early spring-summer transition in the Arctic Ocean

Fernando Puente-Sánchez[1a *], Luis Macías[1b *], Karley L. Campbell[c], Marta Royo[3], Vanessa Balagué[3], Pablo Sánchez[3], Javier Tamames[1], C.J. Mundy[2], and Carlos Pedrós-Alió[1#]

[1] Department of Systems Biology, Centro Nacional de Biotecnología, CSIC, Darwin 3, 28064 Madrid, Spain.

[2] Centre for Earth Observation Science, University of Manitoba, Winnipeg, MB, Canada.

[3] Department of Marine Biology and Oceanography, Institut de Ciències del Mar, CSIC, Ps. Marítim de la Barceloneta 37-49, 08003 Barcelona, Spain.

* These authors contributed equally

[a] Present address: Department of Aquatic Sciences and Assessment, Swedish University for Agricultural Sciences (SLU), Lennart Hjelms väg 9, 756 51, Uppsala, Sweden.

[b] Present address: Aix Marseille Université, CNRS, IRD, College de France, CEREGE, Aix-en-Provence, France.

[c] Present address: UiT, The Arctic University of Norway, Tromsø, Norway.

Corresponding author: cpedros@cnb.csic.es

Abstract

Microbial assemblages under sea ice of Dease Strait, Canadian Arctic, were sequenced for metagenomes and metatranscriptomes of the small size fraction (0.2 to 3 µm). The community from early March was typical for this season, with *Alpha*- and *Gammaproteobacteria* as the dominant taxa, followed by *Thaumarchaeota* and *Bacteroidetes*. Towards summer, *Bacteroidetes* and particularly the genus *Polaribacter*, became increasingly dominant, followed by the *Gammaproteobacteria*. Analysis of genes responsible for microbial acquisition of iron showed an abundance of ABC transporters for divalent cations and ferrous iron. The most abundant transporters, however, were the outer membrane TonB dependent transporters of iron-siderophore complexes. The abundance of iron acquisition genes suggested this element was essential for the microbial assemblage. Interestingly, *Gammaproteobacteria* were responsible for most of the siderophore synthesis genes. On the contrary, *Bacteroidetes* did not synthesize siderophores but accounted for most of the transporters, suggesting a role as cheaters in the competition for siderophores as public goods. Likely, this cheating ability of the *Bacteroidetes* contributed to their dominance in summer.

Introduction

Climate change over the recent decades is evident across the Arctic Ocean through the decline in seasonal sea ice coverage [(1), (2), (3)]. This reduction of sea ice impacts the microorganisms living in the ice and underlying water. For example, a shift towards smaller algae has been observed in phytoplankton [(4)]. The distinctive conditions for life in polar environments involve prolonged periods of ice cover and darkness in winter, generally low water temperatures, and extended irradiance in summer [(5)] The transition from winter to spring and summer involves, thus, dramatic changes in the environment and these are reflected in the composition of the microbial assemblages [(6), (7)]. Prokaryotic taxa abundant in winter such as *Thaumarchaeota* or *Deltaproteobacteria* disappear during the spring, while *Alpha* and *Gammaproteobacteria* and in particular *Bacteroidetes* increase in abundance towards the summer [(8)]. However, the traits that these different microbial taxa use to become dominant are unknown. This is partially due to the logistic difficulties of sampling during the early part of the year. Thus, we carried out a time series through the ice melt transition from early March to late July in Dease Strait of the Canadian Arctic.

Iron is an essential nutrient that is scarce in surface waters due to the insolubility of the most common form Fe(III) and to the fact that sources are of terrestrial origin. As a result, between 15 and 40% of the world's oceans are limited by iron [(9), (10)]. Even in areas where growth is limited by other nutrients (such as the Arctic Ocean) microorganisms need to develop strategies to obtain iron. A common method to get iron in aquatic media is to use siderophores [(11)]. These are small molecular weight compounds that are soluble in water and have a very high affinity for Fe(III). They are

67 synthesized by some microorganisms and usually released in the environment. Then,
68 with the appropriate receptors, the iron-siderophore complexes can be taken up.
69 Siderophores, however, require a complex set of enzymes to be synthesized and
70 excreted in the medium. And, therefore, they require considerable amount of energy
71 [(12)]. Some bacteria do not synthesize siderophores but have the receptors for them.
72 These bacteria act as cheaters, exploiting "public goods" that they have not contributed
73 to create. Due to these peculiarities, the interactions between siderophore producers and
74 non-producers have been explored with cultures of marine *Vibrio* to illustrate
75 competition for public goods [(13)] and the evolutionary implications of these
76 interactions have been reviewed [(14)]. Most experimental information, however, comes
77 from studies with pure cultures of *Proteobacteria*, particularly of different *Vibrio* and
78 *Pseudomonas* strains. But the issue has not been analyzed in nature where the large
79 diversity of coexisting microorganisms may result in complex interactions.
80
81 In the Arctic, *Bacteroidetes* become the most abundant taxon of the assemblage in
82 summer. On the other hand, *Proteobacteria*, that are the most abundant taxa in winter
83 and early spring, decrease in abundance (8). One remarkable difference between
84 *Proteobacteria* and *Bacteroidetes* is the capability to synthesize siderophores.
85 *Proteobacteria* have been shown to synthesize dozens of different siderophores (15),
86 while almost no instances of siderophore synthesis are known among *Bacteroidetes*
87 (16). However, *Bacteroidetes* are known to have receptors for iron-siderophore
88 complexes (17), (18). Therefore, we examine the time evolution of the bacterial
89 assemblage and the presence and abundance of iron-related genes through the ice
90 melting period with the aim to test whether the iron acquisition strategies may have a
91 role in the outcome of the competition among taxa.

Materials and methods

Sampling

Samples were collected in Dease Strait, lower Northwest Passage, Nunavut, Canada (69.03°N, 105.33°W; Figure 1). Water depth was 60 m and samples were collected between 7 March and 24 June 2014, as part of the 2014 Ice Covered Ecosystem-CAMbridge Bay Process Study (ICE-CAMPS). During the ICE-CAMPS campaign, Dease Strait was covered by first-year ice (1.8-2.1 m thick) with drifted snow ranging from 5 to < 25 cm in depth, until melt commenced on 8 June. Snow melt caused the ice surface to flood by 16 June (19), followed by subsequent drainage and the formation of melt ponds that persisted until ice break-up on 19 July. One week after ice break-up, the site was sampled a final time in ice-free waters on 30 July aboard the *R/V Martin Bergmann*.

Water samples were collected opportunistically thirteen times, through a 20-cm diameter hole from 7 to 18 March 2014, protected by a portable tent. For the remainder of the ice-covered season (21 April to 24 June 2014), samples were taken from a 2-m^2 sampling hole maintained within a heated tent. Finally, the 30 July sample was collected, as mentioned, form a ship. A submersible water pump mounted on an under-ice arm was used to collect ice-water interface at 2.5 m. Hydrographic profiles were also taken alongside using a conductivity, temperature and depth probe (RBR XR-620 CTD) equipped with a chlorophyll (chl) *a in vivo* fluorescence sensor. The region is in close proximity to mainland Canada, and receives freshwater inputs from the nearby

117 Coppermine, Hood, Burnside and Ellice rivers (Figure 1). Further details about the
118 study site can be found in Campbell *et al*. (20), (21), (22).
119

120 **Physico-chemical measurements**

121 Approximately at 10 m from the location of water sampling, profiles of under-ice
122 photosynthetically active radiation (PAR) were collected between 10:00 am and 12:30
123 pm local time. This was done using a spherical underwater sensor (LI-193 LI-COR)
124 lowered through an auger hole that took measurements at 1-m depth intervals from the
125 ice-water interface down to 20 m. During measurements the sampling hole was covered
126 to limit contamination by surface radiation. Disturbance of this sites for light
127 measurement was kept to a minimum, where the hole was approached along a single
128 path from the north.
129

130 Following transport to laboratory facilities, water samples that were kept in darkness
131 close to, but not below, -2˚C, and were immediately processed for chl *a* and nucleic
132 acids. Subsamples for chl *a* were filtered onto GF/F filters (Whatmann) before
133 subsequent pigment extraction in 10 ml of 90% acetone for 24 h in darkness and at 4 ˚C.
134 Fluorescence was measured before and after acidification with 5% HCl (Turner Designs
135 Trilogy Fluorometer) according to Parsons et al. (1984) and chl *a* concentration was
136 calculated using the equations of Holm-Hansen et al. (23).
137

138 In order to collect nucleic acids, approximately 10 l of water was prescreened to remove
139 visibly identifiable plankton and then filtered through a tiered stainless steel large-
140 volume filtration system (Millipore) with a succession of 20, 3 and 0.22 µm filters.

141 Separate filters were prepared for RNA and DNA. Filters were immediately frozen at
142 -80˚C. Here we present data from the 0.22 µm filters only.
143

144 **Nucleic acid extraction**

145 DNA was extracted according to the phenol/chloroform protocol detailed by Massana et
146 al. (24). After thawing, frozen filters were cut into small pieces and placed into sterile
147 cryovials. Lysis buffer and lysozyme (final concentration: 1 mg ml^{-1}) were added to the
148 cryovials and they were incubated at 37 °C for 45 min. Sodium dodecyl sulfate (10%)
149 and Proteinase K (0.2 mg ml^{-1}) were added and the mixture was incubated at 55°C for 1
150 h. The lysate was mixed twice with an equal volume of phenol/chloroform/isoamyl
151 alcohol (25:24:1, pH 8) and centrifuged at 12 000 × rpm (10 min). A second extraction
152 with chloroform/IAA (24:1) was carried out to remove the residual phenol. The aqueous
153 phase containing the DNA was concentrated and purified by cleaning up with sterile
154 purified water using Amicon Ultra Centrifugal filters (Millipore). The DNA yield and
155 integrity were quantified in a Nanodrop spectrophotometer (NanoDrop 1000 Thermo
156 Fisher) and Qubit fluorimeter (Thermo Fisher). DNA extracts were stored at -80°C.
157

158 RNA was extracted after cutting the frozen filters into small pieces and using Qiagen's
159 RNeasy kit. After a DNase treatment with Ambion's Turbo DNA-free kit, RNA yield
160 and integrity were quantified with a Nanodrop spectrophotometer (NanoDrop 1000
161 Thermo Fisher) and a Qubit fluorometer (Thermo Fisher). The RNA extracts were
162 stored at -80°C. Prior to sequencing, ribosomal RNA depletion was performed by
163 Sequentia Biotech (http://www.sequentiabiotech.com/) using Illumina's TruSeq
164 Stranded Total RNA LT – with RiboZero.
165

166 **High-throughput sequencing (HTS)**

167 DNA samples were sequenced in two batches. The first batch included most
168 metagenomic samples and was sequenced at CNAG (https://www.cnag.crg.eu) on the
169 Illumina HiSeq2000 sequencing platform using a TruSeq paired-end cluster kit, v3. The
170 second batch included four metagenomic samples (May 10, June 1, June 15, and July
171 30) and all metatranscriptomic samples. The numbers of reads per sample are shown in
172 Supplementary Table S1. We used the SqueezeMeta pipeline (v1.3) and the SQMtools
173 R package (25), (26) for all the bioinformatics analyses. Details of the assembly are
174 shown in Supplementary Table S2. Average gene copy numbers per genome were
175 calculated as described in Puente-Sánchez *et al.*, (26) using the median coverage of 10
176 universal single-copy marker genes (27). These markers are particularly suitable for
177 normalizing metagenomic and metatranscriptomic data to provide estimates of relative
178 per-cell gene copies, because they represent constitutively expressed single-copy
179 housekeeping genes (27). Furthermore, since average copy numbers are normalized
180 against the coverage of well conserved genes, they should be unaffected by the
181 percentage of mapped and/or annotated reads, making them better to compare the
182 abundances of the same function in different samples. Thus, throughout the manuscript
183 we will use average copy numbers per genome when discussing the normalized
184 abundance of individual functions in the microbiome, and percentages of reads assigned
185 to each taxon when discussing taxonomic distributions. Sequences were deposited under
186 NCBI BioProject ID PRJNA803814.
187
188

189 **Taxonomic assignment of ORFs and contigs**

190 For each ORF DIAMOND (v0.9.22) homology searches were performed with its amino
191 acid sequence against the GenBank nr database (downloaded in September, 2019). An
192 e-value cutoff of 1e-03 was set to discard poor hits. The best hit was obtained, and then
193 we selected a range of hits (valid hits) having at least 80% of the bitscore of the best hit,
194 and with an identity to the nr database no smaller than 10% of the identity of the best
195 hit. The Last Common Ancestor (LCA) of all these hits was obtained at diverse
196 taxonomic ranks (from phylum to species). In order to allow for some flexibility, the
197 case of putative transfer events or incorrect annotations in the database, we reported a
198 taxon as the LCA as long as it was supported by 90% of the valid hits.
199
200 To ensure trustworthy annotations we also required a minimum identity to the nr
201 database in order to assign ORFs to the different taxonomic ranks. These identity
202 cutoffs were based on Luo *et al.* (28), and were 85, 60, 55, 50, 46, 42 and 40% for the
203 species, genus, family, order, class, phylum and superkingdom ranks, respectively.
204
205 Finally, for each contig, we obtained a consensus taxonomy from the annotations of all
206 the ORFs encoded in the contig, such as 50% of all the genes (regardless of whether
207 they could be annotated or not) and 70% of the annotated genes belonging to the same
208 taxon. After mapping of the reads to the contigs using Bowtie2 v2.3.4.1 (29), contig
209 taxonomies were used for calculating global taxon abundances in our samples, while
210 ORF taxonomies were used to calculate the taxonomic distribution of particular
211 functions.
212

213 **Functional annotation of open reading frames (ORFs)**

214 The ORFs were functionally annotated into Clusters of Orthologous Groups (COGs) by
215 downloading the eggNOG database (30), selecting the entries annotated as COGs,
216 creating a DIAMOND database and using it for annotation as described in Tamames
217 and Puente-Sánchez (25). COGs were used for functional annotation instead of KEGG
218 orthologs (KOs) or PFAMs, since their finer granularity allowed for a more careful
219 curation of the annotations (see next section).

220

221 **Identification of siderophore synthesis genes and pathways**

222 Pathways for siderophore synthesis usually include two types of enzymes. In the first
223 steps, fairly common enzymes are used, such as for example the protein catalyzing the
224 step chorismate to isochorismate. These enzymes are coded by genes that are common,
225 not only to several siderophore synthesis pathways, but also to more general central
226 metabolic pathways. And next, several additional steps that usually require
227 nonribosomal peptide synthetases (NRPs), polyketide synthases, and NRPs-independent
228 siderophore synthetases (NIS) that condense small and large molecules until the
229 complex structures of the siderophores are completed. In many cases, several of these
230 NRPs are common to different pathways and, thus, different gene names are classified
231 in the same COG category. For example, COG3486 has representatives in at least 13
232 siderophore synthesis pathways (see Supplementary Figure S1). Thus, detecting this
233 COG in metagenomes does not indicate which siderophore pathway is present. On the
234 contrary, some genes are assigned to more than one COG, further complicating the
235 issue. For example, gene *dhbE* in the bacillibactin synthesis pathway is assigned to
236 COGs 0318 (AMP-dependent synthetase and ligase) and COG1021 (2,3-
237 dihydroxybenzoate-AMP ligase). We checked manually all the siderophore synthesis

238 pathways in MetaCyc (31) and added a few more (Supplementary Table S3). We have
239 summarized this complexity in a network (Supplementary Figure S1) that will facilitate
240 identification of both common and unique genes in the synthesis pathways of the
241 different siderophores.
242
243 Since identifying the siderophore pathways that are present in metagenomes and
244 expressed in metatranscriptomes is complicated, we adopted the following criteria:
245 1. In order to state that the pathway for a given siderophore MAY BE present, all
246 the genes in the pathway must be present.
247 2. In order to state that the pathway IS present, there must be a unique gene
248 present, one that is not shared among different pathways.
249 3. If at least one gene of a pathway is absent, we consider the whole pathway
250 absent.
251 There was an additional difficulty. A substantial portion of the genes involved in
252 siderophore synthesis belonged to COG0318. This COG includes genes *entE* in
253 salmochelin and enterobactin pathways (three different steps in the pathways), *pvdI* and
254 *pvdL* in pyoverdin (first condensation step), *dhbE* in bacillibactin (two successive
255 steps), *asbC* in petrobactin (a ligase in two steps), and *acsA* in achromobactin (synthase,
256 four steps). It also includes several enzymes unrelated to siderophore synthesis. Thus,
257 we considered the presence of this COG necessary to fulfill criterion 1 above. However,
258 we did not count the reads assigned to this COG in the quantitation of siderophore
259 synthesis genes, because many of them might code for genes in other metabolic routes.
260 We followed a similar procedure for the rest of the COGs, using for quantitation only
261 those which could be unambiguously assigned to siderophore biosynthesis pathways
262 using the high quality – manually curated SwissProt database (32). Some of them,

263 however, should be involved in siderophore synthesis. Therefore, our counts of

264 siderophore synthesis genes are underestimates.

265

266 **RESULTS**

267

268 ## Changes in ecosystem parameters

269 Daylight increased from <12 h during early March to 24 h in 21 May. The consequent
270 increase in surface irradiance was intensified by the progressive melt of surface snow
271 and ice, with PAR transmitted to 2.5 m depth increasing steadily until 12 June,
272 thereafter, increasing nonlinearly (Figure 2a) as melt ponds formed on the surface. Chl *a*
273 increased steadily throughout the study following the increase in PAR, while salinity
274 decreased slightly at the surface due to ice melting (Figure 2b-c).

275

276 ## Taxonomic composition of the prokaryotic assemblage

277 Microbial populations changed along the study (Figure 3a). In early March
278 *Proteobacteria* dominated the assemblage. Specially, *Alphaproteobacteria* accounted
279 for 36% of the reads and *Gammaproteobacteria* for 20%. The two other main groups
280 were *Taumarchaeota* (12%) and *Bacteroidetes* (9%). Other minor components were
281 *Deltaproteobacteria* (5%), *Actinobacteria* (4%), *Betaproteobacteria* (2.5%),
282 *Verrucomicrobia* (2.5%), *Euryarchaeota* (2.5%), *Planctomycetes* (2%), and
283 *Marinimicrobia* (2%). Progressive changes eventually resulted in a different
284 composition in June. For example, on 23 June the main groups were *Bacteroidetes*
285 (55%), *Alphaproteobacteria* (21%), *Gammaproteobacteria* (18%), chloroplasts (12%),
286 and *Actinobacteria* (2%).

287

288 *Alphaproteobacteria* were, as mentioned, the most abundant group in late winter. The
289 most important orders were *Pelagibacterales* and *Rhodobacterales*, followed by

290 unclassified *Alphaproteobacteria*, and small contributions from *Rhodospirillales* and
291 *Sphingomonadales* (Figure 3b). This is a fairly usual composition in the oceans.
292
293 *Gammaproteobacteria* increased up to 1 June, when they reached 37% of the reads and
294 decreased slightly afterwards (Figure 3a). The most abundant group could not be
295 classified beyond the class level. The next taxa in abundance were *Cand*. Thioglobus
296 and *Cellvibrionales* (Figure 3b). Another unusual group was the Order
297 *Pseudomonadales*. In contrast, *Gammaproteobacteria* groups commonly abundant in
298 the oceans such as SAR86 and *Alteromonadales* had only small contributions.
299
300 Throughout the study, *Flavobacteriales* were the most abundant *Bacteroidetes* order,
301 followed by unclassified *Bacteroidetes*, unclassified *Flavobacteriia*, and *Cytophagales*
302 (Figure 3b). Most of the increment in *Bacteroidetes* was due to the genus *Polaribacter*
303 (Supplementary Figure S2). In effect, at the beginning of the study, the *Bacteroidetes*
304 reads were fairly well distributed among seven taxa: N55, NS9, *Marinoscillum*, NS4,
305 *Polaribacter*, *Owenweeksia* and *Sufflavibacter* in order of abundance and several other
306 minor components. In late June, on the other hand, 60% of the reads belonged to
307 *Polaribacter* and the rest to several other taxa. The increase in *Bacteroidetes* closely
308 followed the phytoplankton summer bloom, as indicated both by chl *a* (Figure 2) and
309 chloroplasts (Figure 3a).
310
311 *Actinobacteria* were present in small amounts throughout the study. Two more bacterial
312 taxa, *Verrucomicrobia* and *Deltaproteobacteria*, were significant at the beginning of the
313 time series, but eventually disappeared. Likewise, the two archaeal phyla
314 *Thaumarchaeota* and *Euryarchaeota* were abundant in March and almost disappeared

315 with the seasonal progression. The bloom of eukaryotic algae in June was reflected as a
316 slight increase in the chloroplast reads towards the end of the study period (Figure 3a).
317

318 **Main iron transport genes**

319 We searched for almost 250 unique genes grouped in 93 COG categories related to iron
320 acquisition and siderophore synthesis (Supplementary Table S3). We pooled the genes
321 into groups with similar functions (Table 1, see scheme in Supplementary Figure S3).
322 Thus, the main transporters of iron were classified into: i) ferrous iron ABC
323 transporters, ii) ferric iron siderophore outer membrane transporters (TonB dependent),
324 and iii) ferric iron ABC transporters. These are the proteins destined to transfer ferrous
325 iron across the cell membrane and ferric iron bound to siderophores across both
326 membranes. Other categories were iv) divalent cation ABC transporters (transporting
327 iron and other cations across the cell membrane), v) transporters of iron bound to
328 dicitrate, vi) transporters of heme groups, vii) storage of iron as ferritin, and viii)
329 regulators of iron metabolism. Finally, we also examined siderophore synthesis genes
330 (see next section).
331

332 Normalized abundance of iron related genes increased from a copy number (CN) of less
333 than 5 in March to higher than 8 in late June (Figure 4a). Thus, the CN of genes devoted
334 to iron acquisition almost doubled along the time series. Three of our categories, ferric
335 iron-siderophore ABC transporters, storage, and siderophore synthesis did not change
336 significantly. Two other, heme and divalent cation ABC transporters increased
337 moderately, while ferric iron TonB dependent, dicitrate and ferrous iron ABC
338 transporters increased substantially. Iron uptake regulation genes also increased and
339 were those with highest CN throughout the study (between 2 and 4, Figure 4a).

340 Globally, regulator genes accounted for about half of the copies in the category, ferric
341 iron (TonB dependent and ABC) for a quarter and the remaining genes for another
342 quarter.
343
344 The taxonomy of these genes generally corresponded to that of the community
345 (compare Figs. 3a and 4b). In other words, the most abundant taxa were responsible for
346 most of the iron related genes. There was only one obvious difference: while
347 *Alphaproteobacteria* were always the first or the second group in abundance, they were
348 always the third one when considering only the iron-related genes, with
349 *Gammaproteobacteria* and *Bacteroidetes* alternating as those with the most genes. This
350 underrepresentation was likely due to the fact that the most abundant member of the
351 *Alphaproteobacteria* was the order *Pelagibacterales* (Figure 3b), that is known to lack
352 all TonB dependent transporters and to have a very small percent of their genome
353 devoted to iron acquisition genes (Cobo-Simón *et al*., in preparation).
354

355 **Ferric iron transport genes**

356 There were large differences in abundance and taxonomy between the outer membrane
357 and cell membrane transporters (Figure 5a and b). The TonB dependent outer
358 membrane transporters increased from a CN of 0.3 in March to reach a maximum of 1.6
359 in late June. Most of this increase was due to *Bacteroidetes* (Figure 5a). In effect, this
360 group accounted for 90% of the reads of these genes in late June. On the contrary, the
361 inner membrane ABC transporters remained almost constant around a CN of 0.9. And
362 the taxonomy was also completely different. In order of importance the main groups
363 were *Alpha*-, *Gammaproteobacteria* and *Bacteoridetes* in the third place (Figure 5b).
364

365 An alternative path to obtain ferric iron is incorporating it bound to dicitrate. The genes
366 for this process increased in parallel to the outer membrane TonB dependent
367 transporters, although at lower CNs (always below 0.6, Supplementary Figure S4a). In
368 this case, *Gammaproteobacteria* and *Bacteroidetes* were responsible for most of the
369 reads.
370
371 The last ferric iron transporter genes that we found were those devoted to transport
372 heme bound iron (Supplementary Figure S4b). These genes also increased with time,
373 mostly due to the *Gammproteobacteria*. *Bacteroidetes* did not have these genes. And
374 towards the end of the study *Actinobacteria* and *Chlorophyta* contributed significantly.
375 The CNs, however, were low, always below 0.15.
376

377 **Siderophore synthesis genes**

378 The CN of siderophore synthesis genes oscillated slightly around 0.025 (Figure 6).
379 These values are likely underestimated because we excluded all the reads of COG0318
380 (see M&M). Still, the CNs are very low compared to the genes to incorporate iron
381 bound to siderophores. Thus, the effort dedicated to siderophore synthesis was
382 moderate, and more or less constant. A portion of these genes could not be assigned to
383 particular bacterial groups. But, of those that could be assigned, most belonged to
384 *Proteobacteria*. Interestingly, *Beta*- and *Deltaproteobacteria* were significant
385 contributors in March, while *Gamma*- and to a lesser extent *Alphaproteobacteria* were
386 the main groups in June. A striking difference with previous groups of genes was that
387 *Bacteroidetes* almost did not contribute anything to siderophore synthesis.
388

389 With the criteria explained in M&M we could confidently state that pathways for eight
390 siderophores were present: alcaligin, enterobactin, mycobactin, myxochelin,
391 petrobactin, salmochelin, and staphyloferrins A and B, and that four were absent
392 (pyochelin, pyoverdin, yersiniabactin, and amphibactin). Again, considering our criteria,
393 the presence of the remaining studied siderophores could not be confirmed
394 (Supplementary Table S4). All eight siderophore synthesis pathways identified as
395 present were found in all the metagenomes except the earliest one on 9 March
396 (Supplementary Table S5).
397

398 **Ferrous iron transport genes**

399 Ferrous iron is able to diffuse through porins into the periplasmic space. There it can be
400 transported to the cytoplasm by ABC transporters, either iron specific or able to transfer
401 several divalent cations including ferrous iron. The ferrous iron specific ABC
402 transporters increased during the study from a copy number of 0.25 to almost 1 in June
403 (Figure 7a). Again, most of the increase was due to *Bacteroidetes* with
404 *Gammaproteobacteria* having a constant contribution. Several other bacterial groups
405 had significant contributions in March and disappeared along the study. These included
406 *Actinobacteria*, *Planctomycetes*, *Verrucomicrobia* and *Gemmatimonadetes*.
407

408 The divalent cation ABC transporters, on the other hand, increased very slightly from a
409 CN of 0.8 to 1.0 (Figure 7b). Interestingly, *Thaumarchaeota*, *Planctomycetes* and
410 *Verrucomicrobia* accounted for half of the reads in March and decreased through
411 spring. *Alphaproteobacteria* accounted for a constant proportion. *Gammaproteobacteria*
412 increased until 15 June and then decreased again. Finally, *Bacteroidetes* had the largest
413 increase becoming dominant in June (70% of the reads).

414

415 ## Other iron related genes

416 We also looked for iron storage genes, mostly related to ferritin (Supplementary Figure
417 S5a). There was only a moderate increase in CN, from 0.2 to 0.3. *Thaumarchaeota* were
418 abundant in March, while *Gammaproteobacteria* and *Bacteroidetes* were abundant in
419 June. Finally, genes involved in the regulation of iron metabolisms were always the
420 most abundant ones (Supplementary Figure S5b), with CNs increasing slightly from 2.1
421 to 3.8 The three most abundant groups of bacteria were also responsible for most of the
422 reads belonging to these genes.

423

424 ## Gene expression

425 Taxonomic assignments of the metatranscriptomic reads are shown in Figs. S6 and S7.
426 On several dates more than half of the reads were either unmapped or unclassified. As a
427 result, the information they provide is limited. Thus, we have only used the
428 metatrancriptomes to show that, considering the mapped and classified reads,
429 expression was proportional to abundance of the taxa. Therefore, there were no
430 differences among the different taxa in the level of expression.

431

432

Discussion

Community composition

The observed change in microbial composition from early spring to summer has previously been reported for the Amundsen Gulf (6), which is approximately 600 km from our study site. The winter community is generally dominated by *Alpha*- and *Gammaproteobacteria*. *Archaea* are important in winter and decrease towards spring and summer (33). Other minor but significant groups in winter are *Betaproteobacteria*, *Verrucomicrobia* and *Actinobacteria*. All of these groups typically decrease and even disappear in summer (8). In contrast, *Bacteroidetes* increase along the spring and become one of the dominant taxa. Predominance of the genus *Polaribacter* is known to be common in polar waters (34). This general structure of groups *Alpha*- and *Gammaproteobacteria* and *Bacteroidetes* dominating is fairly typical of the Arctic Ocean (8), and is supported by this study. This is in contrast to the usual community composition in temperate waters, where *Alphaproteobacteria* are generally dominant accounting for around 50% of the community, and are followed by *Gammaproteobacteria* and *Cyanobacteria*, while *Bacteroidetes* usually account for only 4% and *Betaproteobacteria* are barely detectable (8).

Iron in the Arctic Ocean

There have been several studies determining iron concentrations in the Arctic Ocean. Most of these have been either in the Central Arctic close to the Eurasian coast ((35), (36), concentrations between 0.4 and 0.6 nM) or in the Chuckhi Sea and the Canadian

457 Basin (37), (38), (39), (40). In the Bering Sea, Aguilar-Islas et al. (41) found iron to be
458 limiting in the outer shelf not influenced by ice, but it was sufficient in the outer shelf
459 influenced by ice. This was due to release of dissolved iron from the melting ice. To our
460 knowledge, Colombo *et al*. (42) presented the only study in the Canadian Archipelago.
461 Here, a higher concentration of iron was found than in the deep-water areas to the East
462 and West, with surface concentrations between 0.40 and 1.91 nM above 40 m and
463 between 1.10 and 1.15 between 70 and 100 m. They also noted the well-known inverse
464 correlation between iron concentration and salinity, due to the known influence that
465 freshwater river discharge and ice melt have on enriching sea water in iron. Therefore,
466 iron concentrations in the area are much higher than in most of the oceans. Moreover,
467 N:P ratios in the ice-water interface at our study site suggested nitrogen limitation (21).
468 Thus, iron was not expected to be limiting in these waters. Despite this, iron is an
469 essential nutrient for all microorganisms and it requires special proteins to acquire it.
470 While iron in ocean water could not be directly sampled in this study, our metagenomic
471 data showed presence of iron acquisition genes in all three dominant bacterial taxa, with
472 copy numbers larger than 1 in some cases.
473

474 **Siderophores**

475 In the aerobic ocean, iron is predominantly in the Fe(III) oxidation state, which has a
476 very low solubility and is therefore hard to obtain. One of the most common ways for
477 microorganisms to thus acquire ferric iron is to synthesize siderophores, that can be
478 carried out by many marine microorganisms (11). The chemistry of siderophores in
479 marine microorganisms has been reviewed (43), (44). These studies involve pure culture
480 isolates of marine bacteria in which the siderophores are produced in large enough
481 quantities to be characterized chemically. Most of these belong to

482 *Gammaproteobacteria* genera *Halomonas*, *Vibrio*, *Marinobacter*, *Ochrobacter*,
483 *Pseudoalteromonas*, *Shewanella*, as well as cyanobacteria such as *Synechoccocus* (15).
484
485 Concentrations of siderophores have been measured in a vertical profile at ALOHA
486 station off Hawaii (45), transects from the coast offshore in the southeast Pacific (46),
487 the California Current System (47), and along a latitudinal transect in the oligotrophic
488 Atlantic Ocean (48). In all these studies, ferrioxamines were found in surface waters,
489 while amphibactins were typically more abundant in deep waters and in a high nutrient
490 low chlorophyll zones. Extrapolating this distribution to the costal Arctic, we would
491 expect genes for ferrioxamines but not those of amphibactins in our 60 m deep study
492 region. Actually, we found the whole set of genes for ferrioxamines B and E, which
493 would be in agreement with the previous studies. However, none of these genes was
494 unique to these pathways and, therefore, we cannot assert whether these siderophores
495 were present in our samples or not.
496
497 The pathways for synthesis of amphibactins have not been as well characterized.
498 However, the pathway in *Vibrio neptunius*, a pathogen of bivalve mollusks has been
499 determined (49). We found all the genes for this pathway but one in our metagenomes.
500 Moreover, all the genes found were common to other siderophore synthesis pathways.
501 According to our conservative criteria, amphibactin synthesis pathways were not
502 present in our samples. This would agree with the absence of amphibactins from surface
503 ocean waters. Amphibactins have a polar head with the function of binding iron linked
504 to a fatty acid tail that may be anchored in the outer cell membranes, thus avoiding the
505 dispersion of the siderophore beyond the reach of the producing organism (50) (15).
506 This is a way to avoid utilization of siderophores by alien microorganisms and would

507 seem an adaptive strategy in the oceans. However, as discussed, they do not seem to be
508 abundant in surface marine waters and we did not find the complete pathway in our
509 study.
510

511 **Siderophores in Proteobacteria and Bacteroidetes**

512 *Proteobacteria* is the bacterial phylum in which siderophore synthesis and uptake has
513 been most studied, particularly concerning pathogenic *Gammproteobacteria* (51), (52).
514 In contrast, experimental evidence of siderophore synthesis in *Bacteroidetes* is scarce.
515 Some pathogenic *Flavobacteria* can synthesize siderophores with genes in a plasmid
516 (53). Delmont *et al*. (54) found siderophore synthesis genes in three *Bacteroidetes*
517 metagenomic assembled genomes (MAGs), including two *Polaribacter* and one
518 *Cryomorphaceae,* in a bloom in Antarctica. The *Proteobacteria* MAGs they found did
519 not have these genes. Guan *et al*. (16) found a ferrichrome (*fhuA*) receptor in the fish
520 pathogen *Flavobacterium columnare* that was shown to also synthesize siderophores
521 with the chrome azurol assay. Chen *et al*. (44) reviewed siderophores from marine
522 bacteria and found over 80 of all the known siderophore families. Most siderophores
523 were synthesized by *Gammaproteobacteria* and a few by *Alpha*- and
524 *Betaproteobacteria* and *Actinomycetes*. Only one siderophore was synthesized by a
525 *Bacteroidetes*. This was bisucaberin B made by *Tenacibaculum mesophilum* isolated
526 from a tropical sponge. Fujita *et al*. (55) claimed this was the first siderophore made by
527 a *Bacteroidetes*. In *Allivibrio salmonicida* (*Gammaproteobacteria*) the gene cluster for
528 synthesis and uptake of this siderophore is flanked by transposases. This suggests that
529 this cluster may have been acquired by lateral gene transfer. The same might have
530 occurred in *Tenacibaculum*. Bisucaberin was one of the siderophores that might be
531 synthesized in the Arctic, but the reads did not belong to *Bacteroidetes*.

532

533 On the other hand, there is evidence of *Bacteroidetes* being able to use siderophores
534 made by other bacteria. D'Onofrio *et al*. (17) found that a *Maribacter polysiphoniae* (a
535 member of the family *Flavobacteriaceae*) could grow on solid agar when supplemented
536 with a siderophore from a producer bacterium such as *Microccocus luteus* isolated from
537 the same sediment environment. Zhu *et al*. (18) showed that *Bacteroides*
538 *thetaiotaomicron* could use enterobactin and salmochellin from *E. coli* and
539 *Pseudomonas* in the intestine with *xusABC* genes. Our results are consistent with this
540 model of *Bacteroidetes* contributing very little to synthesis but considerably to uptake
541 of siderophores.

542

543 **Iron-siderophore complexes as common goods**

544 In our Arctic study, the time series followed the development of the seasonal
545 phytoplankton bloom (5), which is triggered by the increasing intensity and duration of
546 solar radiation available (56). In addition to the increased growth of primary producers
547 as ice melts, large amounts of polysaccharides made by ice-algae may be released in the
548 water column (57). For this reason, *Bacteroidetes* are known to grow better when
549 accompanying algal blooms and have a large array of outer cell membrane proteins to
550 take up polysaccharides from them (58), (59). This is likely the main factor in the
551 dominance by *Polaribacter* within this study. However, given the substantial amounts
552 of genes for siderophore uptake and their active expression, it seems that iron was a
553 desirable commodity. Our data on the siderophore synthesis and uptake genes are
554 consistent with competition for siderophores between *Gammaproteobacteria* and
555 *Bacteroidetes*. Both taxa dedicated most iron acquisition genes to the uptake of iron-
556 siderophores. *Bacteroidetes* seemed to act as cheaters while *Gammaproteobacteria* were

synthesizing them. It seems likely that this characteristic, among others, may have helped *Bacteroidetes* to become the most abundant group at the end of the study. Our results confirm the idea of siderophores as public goods, highlight the fact that iron-siderophores are competitively sought after even in environments not limited by iron, and open a fascinating avenue of research for future Arctic cruises.

Author contributions (not necessary in ISME journal)

Study design: C.J. Mundy, CPA.

Sampling and physicochemical data: C.J. Mundy, K. Campbell

Laboratory procedures: Marta Royo, Vanessa Balagué

Raw data processing: P. Sánchez

Data analysis: L. Macías, F, Puente-Sánchez, J. Tamames,

Writing: L. Macías, F. Puente-Sánchez, CPA

All authors contributed to discussion of the results and finalization of the manuscript.

Acknowledgements. Sampling in Dease Strait was funded by an NSERC Discovery and Northern Research Supplement Grant to C.J.M., and in-kind support from the Canadian High Arctic Research Station (CHARS). A. Delaforge assisted greatly in data collection and sample processing. Sequencing and data analysis were funded by grant PID2019-110011RB-C33 from the Agencia Estatal de Investigación of the Spanish Ministerio de Economía y Competitividad to J.T. and C.P.-A. Initial computational analyses were carried out at the Marine Bioinformatics Core facility MARBITS at ICM-CSIC Barcelona, as well as nucleic acid extractions. Most computation and analyses were carried out at CNB.

Compliance with ethical standards

Conflict of interest. The authors declare that they have no conflict of interest.

References

1. Steele M, Ermold W, Zhang J. Arctic Ocean surface warming trends over the past 100 years. Geophys Res Lett. 2008;35(2):1–6.
2. Stroeve J, Notz D. Changing state of Arctic sea ice across all seasons. Environ Res Lett. 2018;13(10).
3. Wang Z, Li Z, Zeng J, Liang S, Zhang P, Tang F, et al. Spatial and Temporal Variations of Arctic Sea Ice From 2002 to 2017. Earth Sp Sci. 2020;7(9):1–20.
4. Li WKW, McLaughlin F a, Lovejoy C, Carmack EC. Smallest algae thrive as the Arctic Ocean freshens. Science [Internet]. 2009 Oct 23 [cited 2013 Mar 19];326(5952):539. Available from: http://www.ncbi.nlm.nih.gov/pubmed/19900890
5. Bunse C, Pinhassi J. Marine Bacterioplankton Seasonal Succession Dynamics. Trends Microbiol [Internet]. 2017;25(6):494–505. Available from: http://dx.doi.org/10.1016/j.tim.2016.12.013
6. Alonso-Sáez L, Sánchez O, Gasol JM, Balagué V, Pedrós-Alio C. Winter-to-summer changes in the composition and single-cell activity of near-surface Arctic prokaryotes. Environ Microbiol. 2008;10(9).
7. Sala MM, Terrado R, Lovejoy C, Unrein F, Pedrós-Alió C. Metabolic diversity of heterotrophic bacterioplankton over winter and spring in the coastal

Arctic Ocean. Environ Microbiol [Internet]. 2008 Apr [cited 2010 Jul 16];10(4):942–9. Available from: http://www.ncbi.nlm.nih.gov/pubmed/18218033

8. Pedrós-Alió C, Potvin M, Lovejoy C. Diversity of planktonic microorganisms in the Arctic Ocean. Prog Oceanogr. 2015;139.

9. Johnson KS, Gordon RM, Coale KH. What controls dissolved iron in the world ocean? Mar Chem. 1997;57:137–61.

10. Moore CM, Mills MM, Arrigo KR, Berman-Frank I, Bopp L, Boyd PW, et al. Processes and patterns of oceanic nutrient limitation. Nat Geosci [Internet]. 2013;6(9):701–10. Available from: http://dx.doi.org/10.1038/ngeo1765

11. Ahmed E, Holmström SJM. Siderophores in environmental research: Roles and applications. Microb Biotechnol. 2014;7(3):196–208.

12. Khan A, Singh P, Srivastava A. Synthesis, nature and utility of universal iron chelator – Siderophore: A review. Vols. 212–213, Microbiological Research. Elsevier GmbH; 2018. p. 103–11.

13. Cordero OX, Ventouras LA, DeLong EF, Polz MF. Public good dynamics drive evolution of iron acquisition strategies in natural bacterioplankton populations. Proc Natl Acad Sci U S A. 2012 Dec 4;109(49):20059–64.

14. Kramer J, Özkaya Ö, Kümmerli R. Bacterial siderophores in community and host interactions. Vol. 18, Nature Reviews Microbiology. Nature Research; 2020. p. 152–63.

15. Vraspir JM, Butler A. Chemistry of marine ligands and siderophores. Vol. 1, Annual Review of Marine Science. 2009. p. 43–63.

16. Guan L, Santander J, Mellata M, Zhang Y, Curtiss R. Identification of an iron acquisition machinery in Flavobacterium columnare. Dis Aquat Organ. 2013

Oct 11;106(2):129–38.

17. D'Onofrio A, Crawford JM, Stewart EJ, Witt K, Gavrish E, Epstein S, et al. Siderophores from Neighboring Organisms Promote the Growth of Uncultured Bacteria. Chem Biol. 2010 Mar 26;17(3):254–64.

18. Zhu W, Winter MG, Spiga L, Hughes ER, Chanin R, Mulgaonkar A, et al. Xenosiderophore Utilization Promotes Bacteroides thetaiotaomicron Resilience during Colitis. Cell Host Microbe. 2020 Mar 11;27(3):376-388.e8.

19. Diaz A, Ehn JK, Landy JC, Else BGT, Campbell K, Papakyriakou TN. The Energetics of Extensive Meltwater Flooding of Level Arctic Sea Ice. J Geophys Res Ocean. 2018 Dec 1;123(12):8730–48.

20. Campbell K, Mundy CJ, Barber DG, Gosselin M. Characterizing the sea ice algae chlorophyll a-snow depth relationship over Arctic spring melt using transmitted irradiance. J Mar Syst [Internet]. 2015;147:76–84. Available from: http://dx.doi.org/10.1016/j.jmarsys.2014.01.008

21. Campbell K, Mundy CJ, Landy JC, Delaforge A, Michel C, Rysgaard S. Community dynamics of bottom-ice algae in Dease Strait of the Canadian Arctic. Prog Oceanogr. 2016 Dec 1;149:27–39.

22. Campbell K, Mundy CJ, Gosselin M, Landy JC, Delaforge A, Rysgaard S. Net community production in the bottom of first-year sea ice over the Arctic spring bloom. Geophys Res Lett. 2017 Sep 16;44(17):8971–8.

23. Holm-Hansen O, Lorenzen CJ, Holmes RW, Strickland JDH. Fluorometric Determination of Chlorophyll. ICES J Mar Sci. 1965;30(1):3–15.

24. Massana R, Balagué V, Guillou L, Pedrós-Alió C. Picoeukaryotic diversity in an oligotrophic coastal site studied by molecular and culturing approaches. FEMS Microbiol Ecol [Internet]. 2004 Nov [cited 2010 Jul 14];50(3):231–43.

656 Available from: http://www.ncbi.nlm.nih.gov/pubmed/19712363
657 25. Tamames J, Puente-Sánchez F. SqueezeMeta, a highly portable, fully
658 automatic metagenomic analysis pipeline. Front Microbiol. 2019;10(JAN):1–
659 10.
660 26. Puente-Sánchez F, García-García N, Tamames J. SQMtools: Automated
661 processing and visual analysis of'omics data with R and anvi'o. bioRxiv.
662 2020;2:1–11.
663 27. Salazar G, Paoli L, Alberti A, Huerta-Cepas J, Ruscheweyh HJ, Cuenca M, et al.
664 Gene Expression Changes and Community Turnover Differentially Shape the
665 Global Ocean Metatranscriptome. Cell. 2019;179(5):1068-1083.e21.
666 28. Luo C, Rodriguez-R LM, Konstantinidis KT. MyTaxa: An advanced taxonomic
667 classifier for genomic and metagenomic sequences. Nucleic Acids Res.
668 2014;42(8):1–12.
669 29. Langmead B, Salzberg SL. Fast gapped-read alignment with Bowtie 2. Nat
670 Methods. 2012;9(4):357–9.
671 30. Huerta-Cepas J, Szklarczyk D, Forslund K, Cook H, Heller D, Walter MC, et al.
672 EGGNOG 4.5: A hierarchical orthology framework with improved functional
673 annotations for eukaryotic, prokaryotic and viral sequences. Nucleic Acids
674 Res. 2016;44(D1):D286–93.
675 31. Caspi R, Billington R, Keseler IM, Kothari A, Krummenacker M, Midford PE, et
676 al. The MetaCyc database of metabolic pathways and enzymes-a 2019
677 update. Nucleic Acids Res. 2020 Jan 1;48(D1):D455–D453.
678 32. Bateman A, Martin MJ, Orchard S, Magrane M, Agivetova R, Ahmad S, et al.
679 UniProt: The universal protein knowledgebase in 2021. Nucleic Acids Res.
680 2021;49(D1):D480–9.

33. Alonso-Sáez L, Waller AS, Mende DR, Bakker K, Farnelid H, Yager PL, et al. Role for urea in nitrification by polar marine Archaea. Proc Natl Acad Sci U S A. 2012;109(44).

34. Ghiglione J-F, Galand PE, Pommier T, Pedrós-Alió C, Maas EW, Bakker K, et al. Pole-to-pole biogeography of surface and deep marine bacterial communities. Proc Natl Acad Sci U S A. 2012 Oct;109(43):17633–8.

35. Klunder MB, Bauch D, Laan P, De Baar HJW, Van Heuven S, Ober S. Dissolved iron in the Arctic shelf seas and surface waters of the central Arctic Ocean: Impact of Arctic river water and ice-melt. J Geophys Res Ocean. 2012;117(1):1–18.

36. Klunder MB, Laan P, Middag R, De Baar HJW, Bakker K. Dissolved iron in the Arctic Ocean: Important role of hydrothermal sources, shelf input and scavenging removal. J Geophys Res Ocean. 2012;117(4):1–17.

37. Nakayama Y, Fujita S, Kuma K, Shimada K. Iron and humic-type fluorescent dissolved organic matter in the Chukchi Sea and Canada Basin of the western Arctic Ocean. J Geophys Res Ocean. 2011;116(7):1–16.

38. Aguilar-Islas AM, Rember R, Nishino S, Kikuchi T, Itoh M. Partitioning and lateral transport of iron to the Canada Basin. Polar Sci [Internet]. 2013;7(2):82–99. Available from: http://dx.doi.org/10.1016/j.polar.2012.11.001

39. Hioki N, Kuma K, Morita Y, Sasayama R, Ooki A, Kondo Y, et al. Laterally spreading iron, humic-like dissolved organic matter and nutrients in cold, dense subsurface water of the Arctic Ocean. Sci Rep. 2014;4:1–9.

40. Kondo Y, Obata H, Hioki N, Ooki A, Nishino S, Kikuchi T, et al. Transport of trace metals (Mn, Fe, Ni, Zn and Cd) in the western Arctic Ocean (Chukchi

Sea and Canada Basin) in late summer 2012. Deep Res Part I Oceanogr Res Pap. 2016 Oct 1;116:236–52.

41. Aguilar-Islas AM, Rember RD, Mordy CW, Wu J. Sea ice-derived dissolved iron and its potential influence on the spring algal bloom in the Bering Sea. Geophys Res Lett. 2008;35(24):10–4.

42. Colombo M, Jackson SL, Cullen JT, Orians KJ. Dissolved iron and manganese in the Canadian Arctic Ocean: On the biogeochemical processes controlling their distributions. Geochim Cosmochim Acta. 2020 May 15;277:150–74.

43. Sandy M, Butler A. Microbial iron acquisition: Marine and terrestrial siderophores. Chem Rev. 2009 Oct 14;109(10):4580–95.

44. Chen J, Guo Y, Lu Y, Wang B, Sun J, Zhang H, et al. Chemistry and biology of siderophores from marine microbes. Vol. 17, Marine Drugs. MDPI AG; 2019.

45. Bundy RM, Boiteau RM, McLean C, Turk-Kubo KA, McIlvin MR, Saito MA, et al. Distinct siderophores contribute to iron cycling in the mesopelagic at station ALOHA. Front Mar Sci. 2018 Mar 1;5(MAR).

46. Boiteau RM, Mende DR, Hawco NJ, McIlvin MR, Fitzsimmons JN, Saito MA, et al. Siderophore-based microbial adaptations to iron scarcity across the eastern Pacific Ocean. Proc Natl Acad Sci U S A. 2016 Dec 13;113(50):14237–42.

47. Boiteau RM, Till CP, Coale TH, Fitzsimmons JN, Bruland KW, Repeta DJ. Patterns of iron and siderophore distributions across the California Current System. Limnol Oceanogr. 2019 Jan 1;64(1):376–89.

48. Mawji E, Gledhill M, Milton JA, Tarran GA, Ussher S, Thompson A, et al. Hydroxamate siderophores: Occurrence and importance in the Atlantic Ocean. Environ Sci Technol. 2008 Dec 1;42(23):8675–80.

731 49. Galvis F, Ageitos L, Martínez-Matamoros D, Barja JL, Rodríguez J, Lemos ML,
732 et al. The marine bivalve molluscs pathogen Vibrio neptunius produces the
733 siderophore amphibactin, which is widespread in molluscs microbiota.
734 Environ Microbiol. 2020 Dec 1;22(12):5467–82.
735 50. Martinez JS, Butler A. Marine amphiphilic siderophores: Marinobactin
736 structure, uptake, and microbial partitioning. J Inorg Biochem. 2007
737 Nov;101(11–12):1692–8.
738 51. Porcheron G, Garénaux A, Proulx J, Sabri M, Dozois CM. Iron, copper, zinc,
739 and manganese transport and regulation in pathogenic Enterobacteria:
740 Correlations between strains, site of infection and the relative importance of
741 the different metal transport systems for virulence. Front Cell Infect
742 Microbiol. 2013;3(DEC):1–24.
743 52. Holden VI, Bachman MA. Diverging roles of bacterial siderophores during
744 infection. Metallomics. 2015 Jun 1;7(6):986–95.
745 53. Møller JD, Ellis AE, Barnes AC, Dalsgaard I. Iron acquisition mechanisms of
746 Flavobacterium psychrophilum. J Fish Dis. 2005;28(7):391–8.
747 54. Delmont TO, Murat Eren A, Vineis JH, Post AF. Genome reconstructions
748 indicate the partitioning of ecological functions inside a phytoplankton
749 bloom in the Amundsen Sea, Antarctica. Front Microbiol. 2015;6(OCT).
750 55. Fujita MJ, Nakano K, Sakai R. Bisucaberin B, a linear hydroxamate class
751 siderophore from the marine bacterium tenacibaculum mesophilum.
752 Molecules. 2013;18(4):3917–26.
753 56. Back DY, Ha SY, Else B, Hanson M, Jones SF, Shin KH, et al. On the impact of
754 wastewater effluent on phytoplankton in the Arctic coastal zone: A case
755 study in the Kitikmeot Sea of the Canadian Arctic. Sci Total Environ

[Internet]. 2021;764:143861. Available from: https://doi.org/10.1016/j.scitotenv.2020.143861

57. Niemi A, Meisterhans G, Michel C. Response of under-ice prokaryotes to experimental sea-ice DOM enrichment. Aquat Microb Ecol. 2014;73(1):17–28.

58. Fernández-Gómez B, Richter M, Schueler M, Pinhassi J, Acinas SG, González JM, et al. Ecology of marine Bacteroidetes: a comparative genomics approach. ISME J. 2013 May;7(5):1026–37.

59. Reintjes G, Fuchs BM, Scharfe M, Wiltshire KH, Amann R, Arnosti C. Short-term changes in polysaccharide utilization mechanisms of marine bacterioplankton during a spring phytoplankton bloom. Environ Microbiol. 2020;22(5):1884–900.

769

770

771 **Table 1**. Categories of iron transport and siderophore synthesis genes used in the present

772 paper.

Category	Function	Transporter type	Location	Examples
Fe(II)	ferrous iron transport	ABC	Cell membrane	*efeUOB*
Fe(III)-OM	ferric iron +sideorphore transport	TonBD	Outer membrane	*fhuA*
Fe(III)-CM	ferric iron +sideorphore transport	ABC	cell	*fhuBCD*
Divalent cation	divalent cations transport including iron	ABC	cell	*sitABC*
Dicitrate	iron + dicitrate transport	TonBD, ABC	out, cell	*fecABCD*
Heme	iron + heme transport	TonBD, ABC	out, cell	*hemR, hemUV*
Storage	ferritin	-	cytoplasm	*bfr*
Regulators	regulation of iron related genes	-	cytoplasm	*fur, irr*
Siderophore synthesis	Synthesis of siderophores	-	cytoplasm	*entABCDF*

773

774

FIGURES

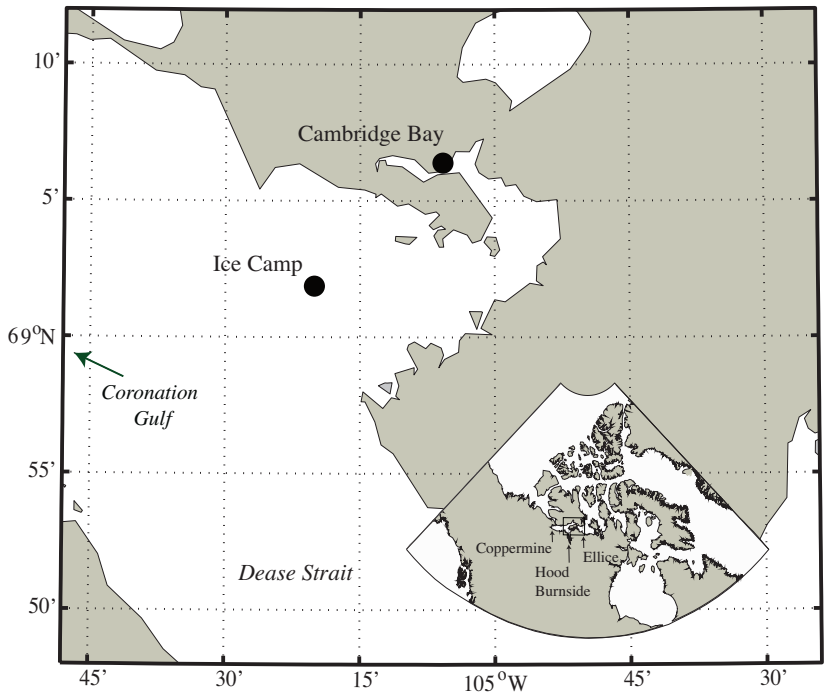

Figure 1. Map of study location near Cambridge Bay, Nunavut. Inset includes approximate locations of the main rivers in the area.

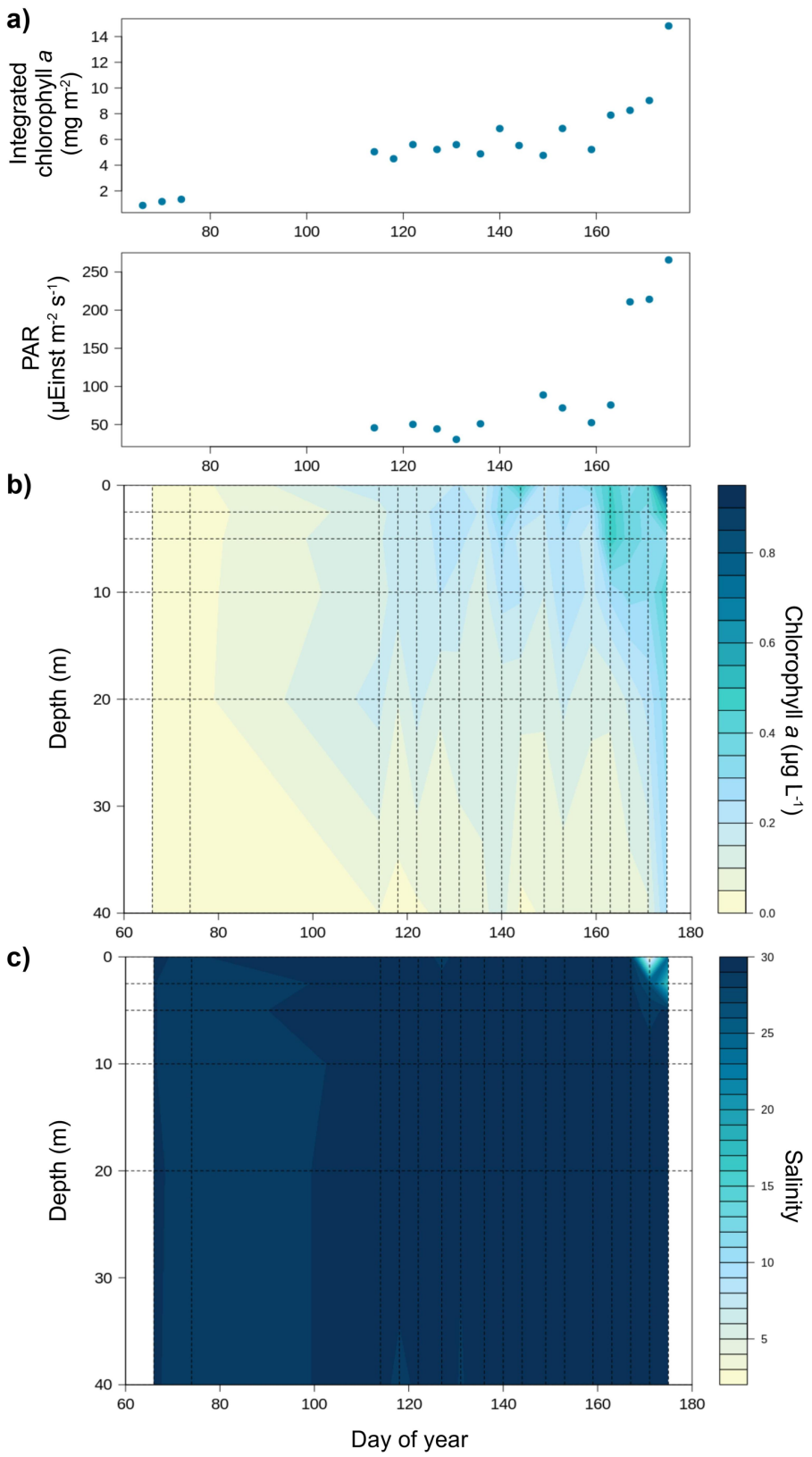

Figure 2. (a) Integrated chlorophyll *a* (mg m^{-2}) and PAR (µEinst m^{-2} s^{-1}) along day of year. (b) Time-depth diagram of chlorophyll *a* (µg L^{-1}). (c) Time-depth diagram of salinity (‰).

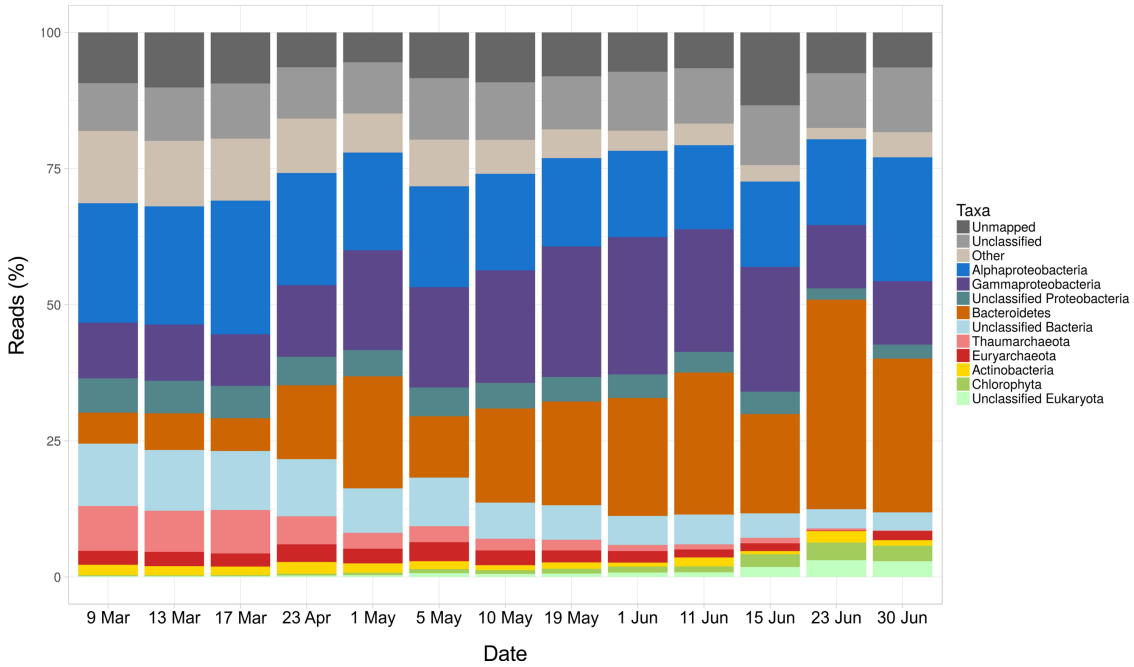

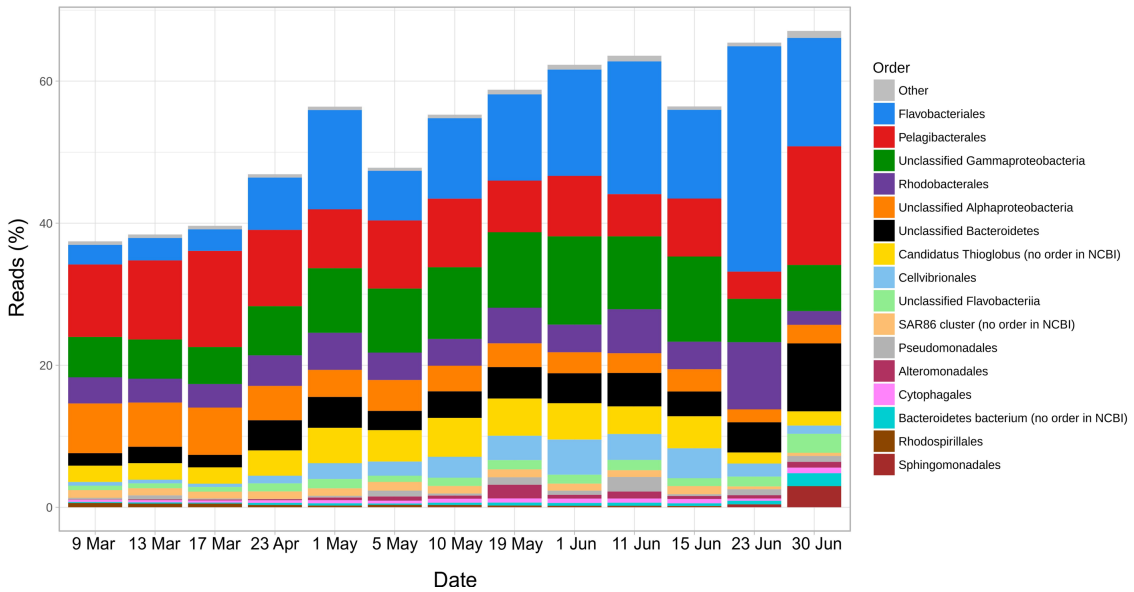

Figure 3. Percent of reads in metagenomes at two different taxonomic levels: phyla and Proteobacteria classes (a) and orders (b).

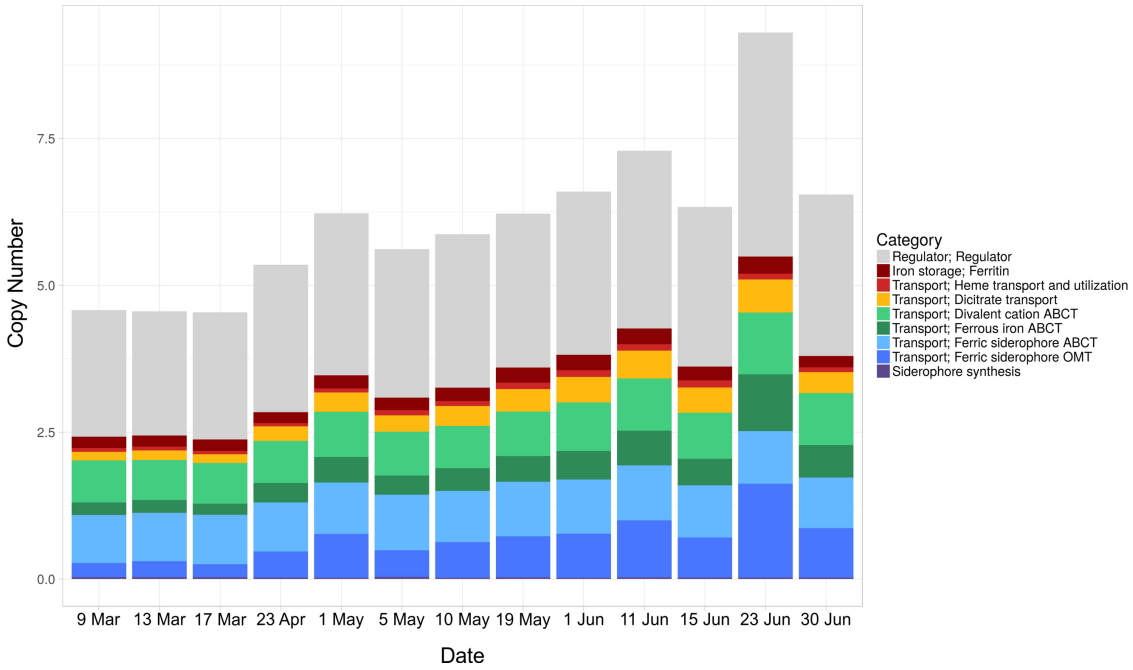

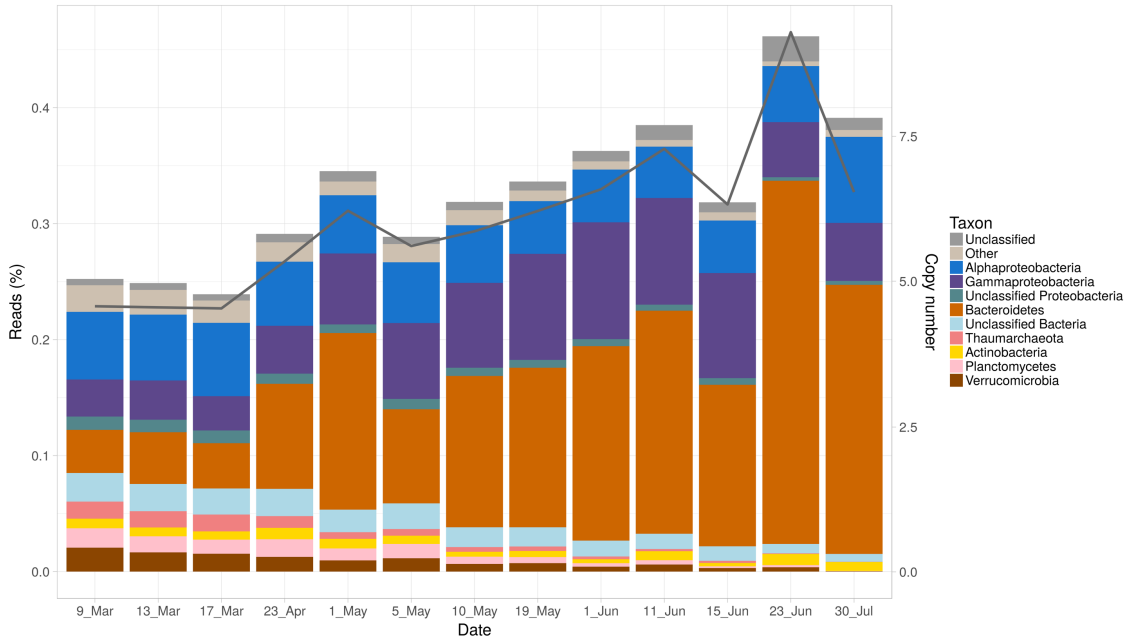

Figure 4. (a) Copy numbers of iron related genes through the study period in metagenomes. (b) Percent of the reads assigned to different taxonomic groups (bars, left hand scale) and copy numbers (line and right hand scale). **(b).** Taxonomy of iron related genes.

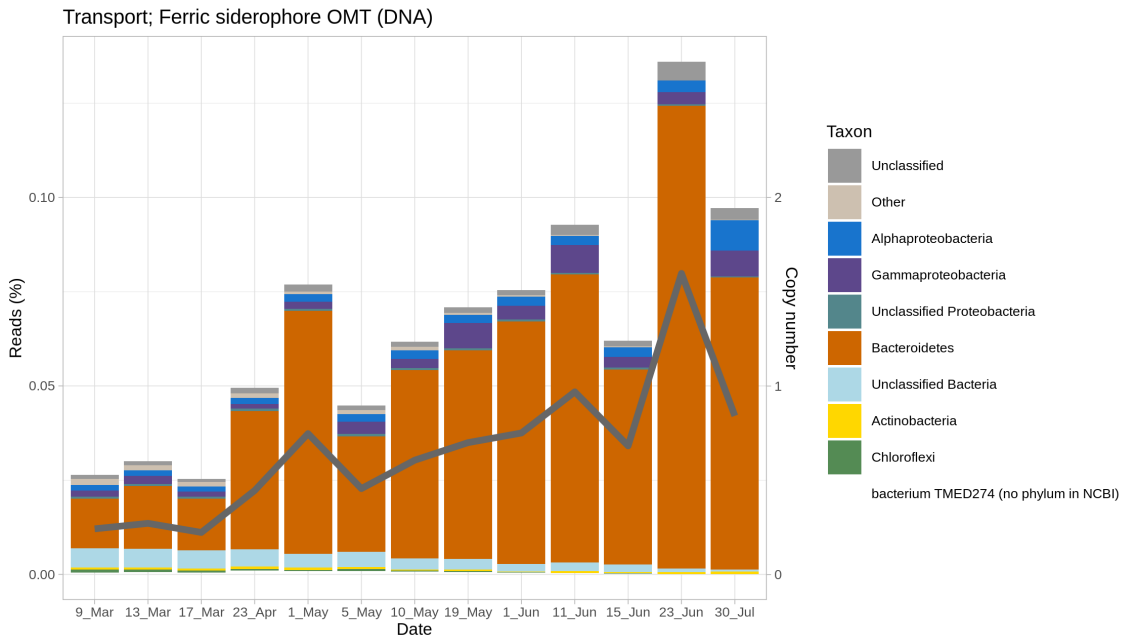

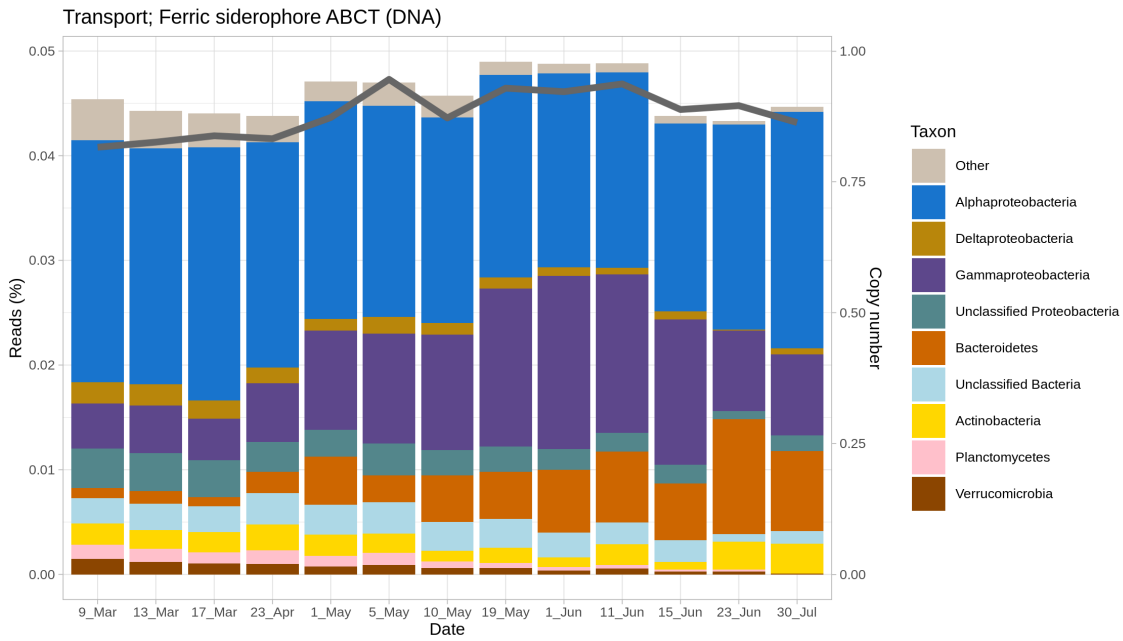

Figure 5. Taxonomic assignments and copy numbers of ferric iron transporter genes along the study: outer membrane ferric siderophore TonBD (above) and cell membrane ABC (below).

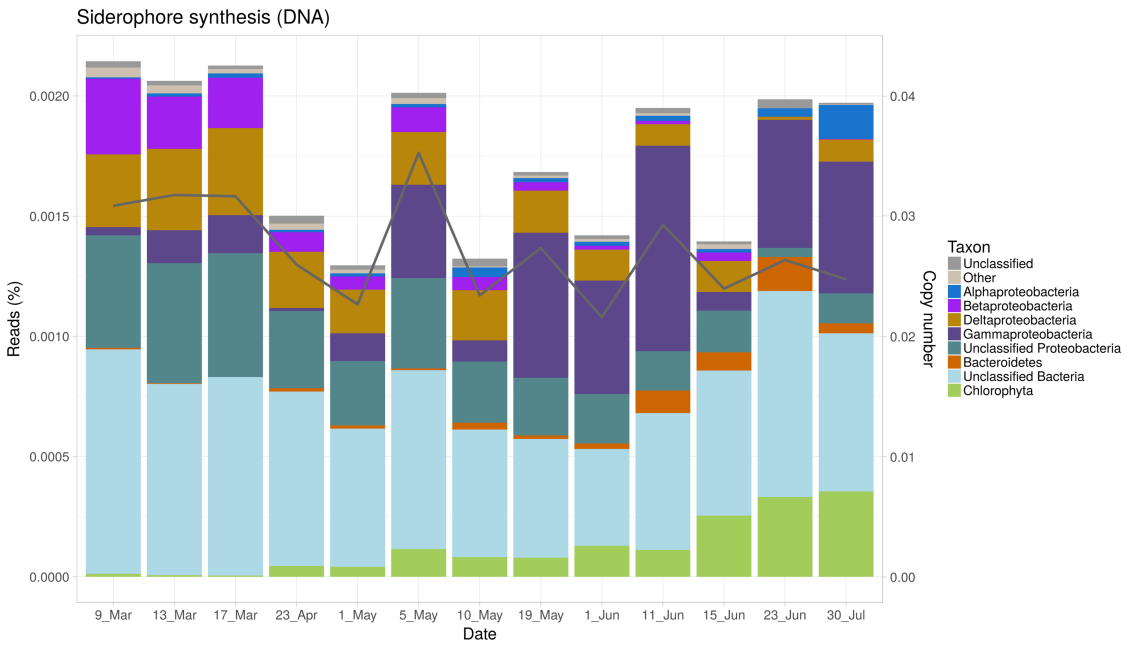

Figure 6. Taxonomic assignments (bars) and copy numbers (line and right scale) of siderophore synthesis genes.

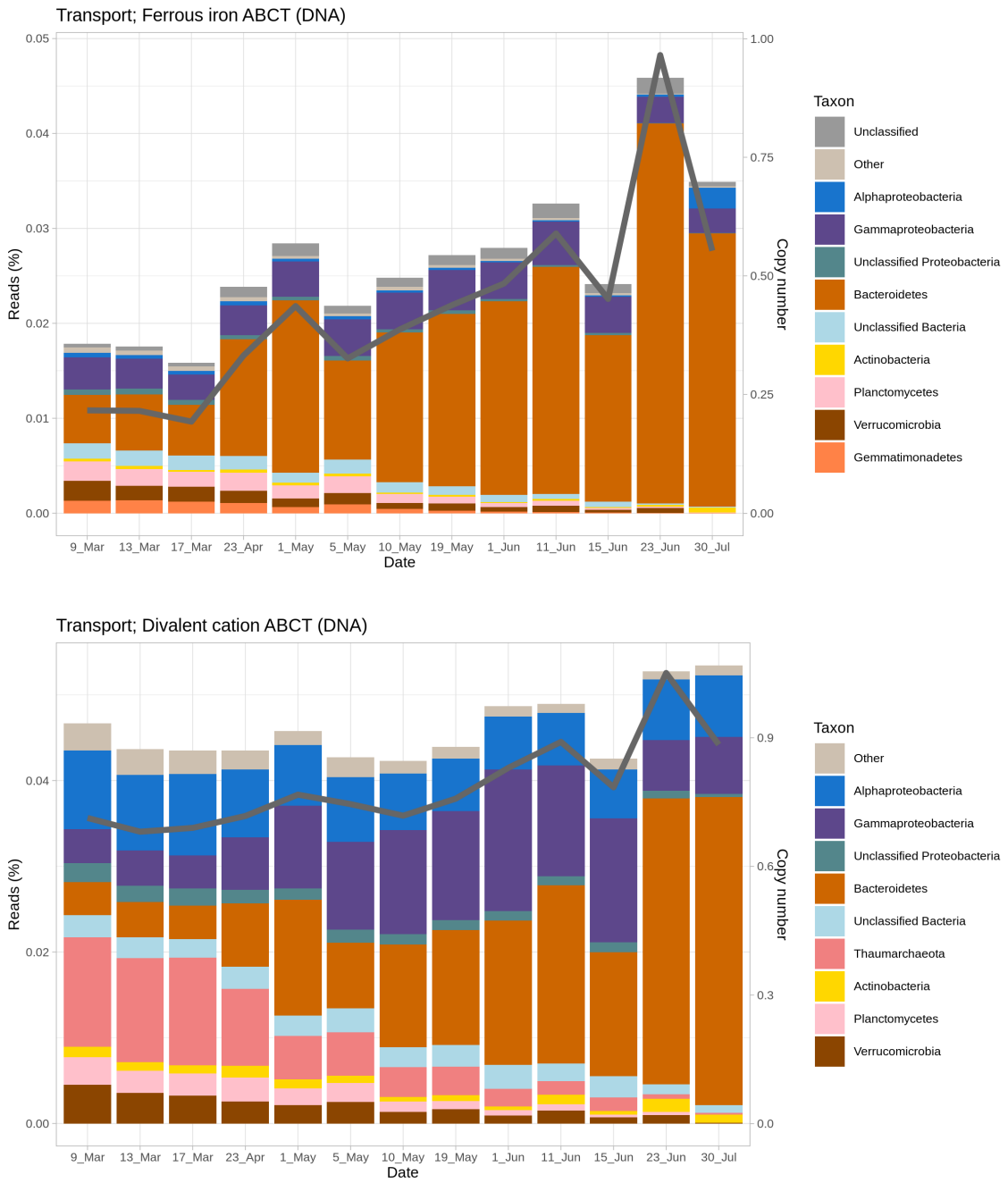

Figure 7. Taxonomic assignments and copy numbers of (a) ferrous iron ABC transporter genes and (b) divalent cation ABC transporter genes along the study.